UNIVERSITI TEKNOLOGI MARA

MATHEMATICS AND STATISTICS

UNDERGRADUATE RESEARCH PROCEEDINGS 2025

UiTM CAWANGAN NEGERI SEMBILAN

Numerical Solution of Unsteady Boundary Layer Flow Over a Stretching Sheet in a Porous Medium Using BVP4C

Nurul Ain Ashiqin binti Ahmad Tarmizi[1,*] and Dr Siti Hidayah binti Muhad Saleh[1]
[1] *College of Computing, Informatics and Mathematics, Universiti Teknologi MARA, 70300, Seremban, Negeri Sembilan, Malaysia*
[*]2023389991@student.uitm.edu.my

Abstract

The movement of fluid within a porous medium plays a pivotal role in various industrial applications including water circulation in geothermal reservoirs, nuclear waste storage, food processing and others. Nonetheless, examining unsteady boundary layer flow in a stretching sheet over a porous medium presents a complex interplay of nonlinear differential equations influenced by multiple external factors. This study also incorporates the effects of velocity and thermal slip to provide deeper insights. By applying similarity transformation, the governing non-linear partial differential equations were transformed into a system of nonlinear ordinary differential equations. Subsequently, the ordinary differential equations were numerically solved using the BVP4C method within MATLAB software. Numerical results are presented for the dimensionless velocity profile, temperature profile, skin friction coefficients and the local Nusselt number under varying parameter conditions. Following that, the results were validated by comparing the BVP4C method with other established numerical methods ensuring the reliability of the findings. The findings indicate that an increase in the permeability parameter leads to a decreased velocity profile and skin friction coefficient while simultaneously enhancing the temperature profile and the local Nusselt number.

Keywords*:* unsteady flow, porous medium, stretching sheet, BVP4C

1. Introduction

The theory of boundary layer flow was first introduced by Ludwig Prandtl who is German scientist [1]. The study was a significant development in understanding the fluid behaviour around solid object since he has made it necessary to analyze more simply. This flow can be categorized into steady and unsteady states depending on whether the fluid properties remain constant or change over time. Therefore, this study focuses on unsteady boundary layer flow and heat transfer in a porous medium that may be found in nature such as soil, road pavement, petroleum reservoirs, biological tissues, print paper, wood, and nanostructured materials [2].

To analyze unsteady boundary layer flow over porous media, numerical techniques such as the BVP4C method are employed. BVP4C stands for boundary value problem for ordinary differential equations with fourth-order accuracy is a reliable numerical solver that handles complex fluid flow problems with boundary conditions specified at multiple points. This method is particularly useful for higher-order differential equations that do not have closed-form analytical solutions, making it widely applicable in engineering, physics, and biological studies [3]. Researchers have extensively used BVP4C to investigate various fluid dynamics problems, including unsteady magnetohydrodynamic (MHD) flows, nanofluid interactions, and convective heat transfer in porous media as seen in [4] and [5].

Numerous studies have examined unsteady MHD flow over porous surfaces using different analytical and numerical techniques. From [6] and [7], they analyzed Casson fluid over a vertical porous plate using the Galerkin finite element method and Laplace transform method, respectively, highlighting how heat source parameters influence velocity and temperature profiles. Similarly, [8] studied unsteady MHD nanofluid flow over a rotating and stretchable disk using the shooting method and the fourth-order Runge-Kutta-Fehlberg method, demonstrating how magnetic parameters affect velocity and temperature. Other researchers have utilized analytical solutions, such as the optimal auxiliary function method [9] and the conformal map method [10] to study porous medium flow under various conditions.

For numerical approaches, methods like the finite difference method in [11] and [12], Fibonacci wavelet series collocation method [13] while Keller-box method [14] have been employed to investigate unsteady MHD flow in porous media. Studies have shown that fluid velocity and temperature distributions are significantly affected by parameters such as porosity, magnetic fields, and heat sources [15]. BVP4C has been extensively applied in research involving biological systems, such as nanofluid flow with injected nanoparticles in arteries [16] and heat transfer in hybrid nanoparticles within divergent channels [17].

Therefore, this study aims to further analyze on unsteady boundary layer flow over a porous stretching sheet conducted using the BVP4C method [18]. The findings will contribute to a deeper understanding of heat transfer and fluid dynamics in engineering applications, particularly in the fields of aerodynamics, energy systems, and biomedical engineering.

2. Methodology

The unsteady boundary layer flow occurred in the porous medium under the conditions of stretching sheet shown in Figure 1. The diagram applied Cartesian coordinate system with the origin marked as O was the stagnation point where the velocity of fluid was zero because of high pressure.

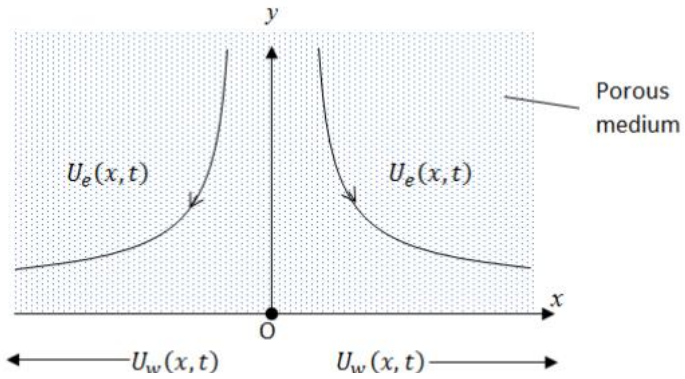

Figure 1: Physical Model of Flow and Coordinate System [18].

The arrows denoted as $U_e(x,t) = \dfrac{ax}{(1-\alpha t)}$ defined as stagnation flow velocity where $a > 0$ represent as the straining parameter and α is a constant. The direction showed that the velocity decreased as it entered the porous medium and moved away from the y-axis. Next, the arrows

represented as $U_W(x,t) = \dfrac{cx}{(1-\alpha t)}$ indicated as the stretching velocity where the $c > 0$ defined as stretching parameter. The direction displayed that the fluid flow moved along the x-axis.

The governing equations in unsteady boundary layer flow defined as the mathematical equations that represented behaviour of fluid. The equations were in the form of partial differential equations which contain more than one variable. There were three fundamental equations which are Eq. (1) - (3) and the boundary conditions in Eq. (4).

Conservation of continuity:

$$\frac{\partial u}{\partial x} + \frac{\partial v}{\partial y} = 0, \tag{1}$$

Conservation of momentum:

$$\frac{\partial u}{\partial t} + u\frac{\partial u}{\partial x} + v\frac{\partial u}{\partial y} = \frac{\partial U_e}{\partial t} + U_e\frac{\partial U_e}{\partial x} + \nu\frac{\partial^2 u}{\partial y^2} + \frac{\nu}{K_1}\left(U_e - u\right), \tag{2}$$

Conservation of energy:

$$\frac{\partial T}{\partial t} + u\frac{\partial T}{\partial x} + v\frac{\partial T}{\partial y} = \frac{k}{\rho c_p}\frac{\partial^2 T}{\partial y^2}, \tag{3}$$

Boundary conditions:

$$u = U_W(x,t) + N_1\nu\left(\frac{du}{dy}\right),$$

$$v = 0,$$

$$T = T_W + D_1\left(\frac{dT}{dy}\right) \text{ at } y = 0. \tag{4}$$

$$u \to U_e(x,t),$$

$$T \to T_\infty \text{ as } y \to \infty.$$

where:

u, v = velocity along x and y axis

T = temperature of fluid

K_1 = the permeability of the porous medium

$\nu = \frac{\mu}{\rho}$ = kinematic viscosity

μ = dynamic viscosity

ρ = density of fluid

k = thermal conductivity of fluid

t = time

c_p = specific heat.

Then, the velocity and thermal slip and were changes throughout time in the way described below in Eqs. (5) and (6)

$$N_1 = N(1-\alpha t)^{\frac{1}{2}}, \tag{5}$$

$$D_1 = D(1-\alpha t)^{\frac{1}{2}}, \tag{6}$$

where:

N = initial values of velocity

D = thermal slip factors.

Furthermore, the surface temperature was provided by Eq. (7)

$$T_W(x,t) = T_\infty + T_O\left(\frac{cx^2}{2\nu}\right)(1-\alpha t)^{\frac{1}{2}}, \tag{7}$$

where:

T_w = wall temperature

T_∞ = free stream temperature

T_o = rate of temperature increases along the sheet (constant).

Moreover, the similarity variables are provided by Eqs. (8) – (10)

$$\eta = y\sqrt{\frac{c}{v(1-\alpha t)}}, \tag{8}$$

$$\psi = y\sqrt{\frac{cv}{(1-\alpha t)}}x\, f(\eta), \tag{9}$$

$$T = T_\infty + (T_W - T_\infty)\theta(\eta), \tag{10}$$

where:

η = boundary layer thickness

ψ = stream function

T = temperature.

By substituting the similarity variables Eqs. (8) – (10) and implement the derivation process has transformed the equation Eqs. (1) – (4) into ordinary differential equations as shown in Eqs. (11) – (13)

Conservation of momentum:

$$f'''(\eta) + f(\eta)f''(\eta) - [f'(\eta)]^2 - A\left[\frac{\eta}{2}f''(\eta) + f'(\eta) - b\right] + b^2 + K\left[b - f'(\eta)\right] = 0, \tag{11}$$

Conservation of energy:

$$\frac{1}{Pr}\theta'' + f(\eta)\theta'(\eta) - 2f'\theta - \frac{A\left(3\theta + \eta\theta'\right)}{2} = 0, \tag{12}$$

where the unsteadiness parameter $A = \frac{\alpha}{c}$ and velocity ration parameter $b = \frac{\alpha}{c}$.

Boundary conditions:

$$f'(0) = 1 + \lambda f''(0),$$

$$f(0) = 0,$$

$$\theta(\eta) = 1 + \delta\theta'(\eta). \tag{13}$$

$$f'(\eta) \to b,$$

$$\theta(\eta) \to 0 \quad \text{as} \quad \eta \to \infty.$$

where $\lambda = N(cv)^{\frac{1}{2}}$ is the velocity slip parameter and $\delta = D_1\left(\frac{c}{v}\right)^{\frac{1}{2}}$ is thermal slip parameter.

After that, the physical quantity of interest that have examined in this study are the skin friction coefficient and local Nusselt number in Eqs. (14) and (15)

Skin friction coefficient:

$$C_f = \frac{\tau_w}{\rho(U_e)^2} \text{ where } \tau_w = \mu\left(\frac{\partial u}{\partial y}\right)_{y=0}, \tag{14}$$

which τ_w defined as the shear stress.

Local Nusselt number:

$$Nu_x = \frac{xq_w}{k(T_w - T_\infty)} \text{ where } q_w = -k\left(\frac{\partial T}{\partial y}\right)_{y=0}, \tag{15}$$

which q_w defined as the surface heat.

Using the similarity variables, the skin friction coefficient and local Nusselt number convert into Eqs. (16) and (17)

$$(b)^{\frac{3}{2}} C_f \left(Re_x\right)^{\frac{1}{2}} = f''(0), \tag{16}$$

$$\sqrt{b}\,Pr^{\frac{1}{2}}\,Nu_x = -\theta'(\eta)Pe_x^{\frac{1}{2}}, \tag{17}$$

where the local Reynolds number denotes as $Re_x = \frac{U_e x}{v}$, Prandtl number $Pr = \frac{\mu c_p}{k}$ and local Peclet number is $Pe_x = U_e x \frac{1}{\alpha_m}$ with α_m is the thermal diffusivity.

3. Result and Discussion

Subsequently, numerical approach using the BVP4C method is applied to solve the ordinary differential equation Eqs. (11) and (12) with the boundary conditions Eq. (13). Firstly, create a function that declare all the necessary variables that are include in the ODEs represent as the 'odefun' function and also define 'bcfun' code for the boundary conditions. Then, create an initial guess for the solution using 'bvpinit' function. This function also involves the process of discretization or separates the domain of the independent variable such as time into a mesh or grid of points. After that, call the 'bvp4c' function to solve the boundary value problem by passing the first-order ODE function, boundary conditions function and the initial guess in the form of piece-wise continuous polynomial. The following shows the transformed first order equations in Eqs. (18) – (20)

$$y_1 = f, \quad y_2 = f', \quad y_3 = f'',$$

$$y_4 = \theta, \quad y_5 = \theta'.$$

$$\frac{dy_1}{d\eta} = f' = y_2.$$

$$\frac{dy_2}{d\eta} = f'' = y_3.$$

$$\frac{dy_3}{d\eta} = f''' = -y_1 y_3 + \left[y_2\right]^2 + A\left[\frac{\eta}{2}y_3 + y_2 - b\right] - b^2 - K\left[b - y_2\right]. \tag{18}$$

$$\frac{dy_4}{d\eta} = \theta' = y_5.$$

$$\frac{dy_5}{d\eta} = \theta'' = Pr\left[-y_1 y_5 + 2y_2 + \frac{A\left(3y_4 + \eta y_5\right)}{2}\right]. \tag{19}$$

$$y_{a1} = 0, \quad y_{a2} = 1 + \lambda y_{a3}, \quad y_{a4} = 1 + \delta y_{a5}, \qquad y_{b2} = 0, \quad y_{b4} = 0. \tag{20}$$

Furthermore, the comparison of the present study was examined to ensure the validity of the numerical solution procedure used. The comparison on skin friction coefficient $f''(0)$ of steady boundary layer flow with no slip effects for different values of velocity ratio parameter b when $A = K = \lambda = \delta = 0$ are tabulated in Table 1. From this table, it indicates that a strong agreement with these methods which confirm the validation of the implemented method.

Table 1: Comparison of results of skin fiction coefficients $f''(0)$ for several values of b when $A = K = 0$ for steady flow and $\lambda = \delta = 0$ with no slip condition

b	**Nazar et al. (2004) Keller-Box Method**	**Rosali et al. (2020) Shooting Method**	**Present Result BVP4C Method**
0.01	-0.9980	-0.998065	-0.998403828
0.02	-0.9958	-0.995811	-0.996083557
0.05	-0.9876	-0.987588	-0.987729976
0.10	-0.9694	-0.969457	-0.969436241
0.20	-0.9181	-0.918118	-0.918113199
0.50	-0.6673	-0.667264	-0.667263682
2.00	2.0176	2.017503	2.017502790
3.00	4.7296	4.729282	4.729282329

Afterward, the effects of the permeability parameter K, velocity slip parameter λ and thermal slip parameter δ were investigated on velocity profile, temperature profile as well as non-dimensional quantities which are skin friction coefficients and local Nusselt number. Graphical representations of the results are used to demonstrate the behaviours of the flow and heat transfer.

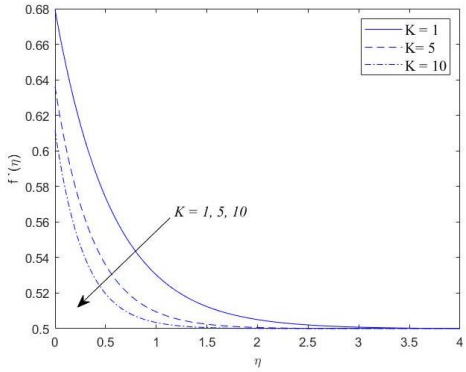

Figure 2: Velocity profile $f'(0)$ for different values of K when $Pr = 0.7$, $A = 1$, $\lambda = 1$, $\delta = 0$ and $b = 0.5$.

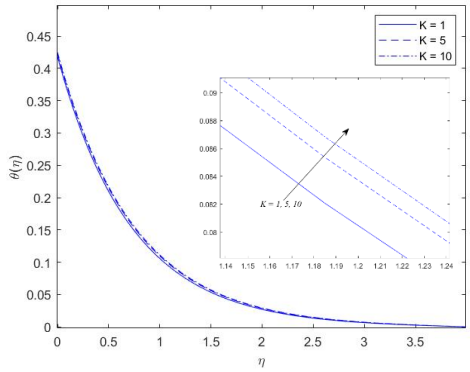

Figure 3: Temperature profile $\theta(0)$ for different values of K when $Pr = 0.7$, $A = 1$, $\lambda = 1$, $\delta = 0$ and $b = 0.5$.

Figure 2 and Figure 3 show the influence of various permeability parameter K on velocity and temperature profiles. Figure 2 indicates that the velocity decrease by the increasing values of K. Based on physical interpretation, the existence of porous medium has increases resistance to fluid flow thereby reducing the overall movement within boundary layer. From Figure 3, it is obvious show that the presence of porous medium increases the temperature profile. This indicates that the temperature decreases as the thickness of thermal boundary layer far away from the surface with the consistent heat transfer into the surrounding medium.

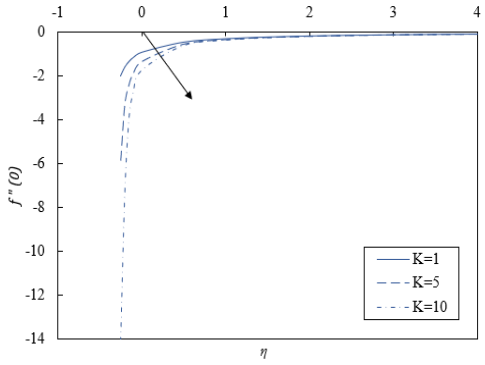

Figure 4: Skin friction coefficient $f''(0)$ for different values of K when $Pr = 0.7$, $A = 1$, $\lambda = 1$, $\delta = 1$ and $b = 0.5$.

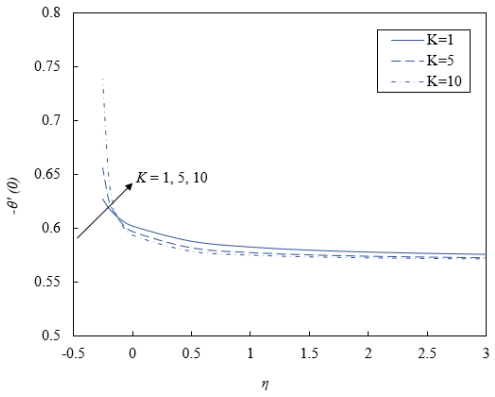

Figure 5: Local Nusselt number $-\theta'(0)$ for different values of K when $Pr = 0.7$, $A = 1$, $\lambda = 1$, $\delta = 1$ and $b = 0.5$.

Figure 4 show that the skin friction coefficients decrease as permeability parameter K increases. The values of the skin friction coefficient approach certain values with the increase in the value of velocity slip parameter λ for different values of permeability parameter K. It can be observed that the effect of permeability parameter K is small for large values of velocity slip parameter λ. Next, Figure 5 demonstrates a trend as the permeability parameter K increases, the local Nusselt number also increases. Based on physical perspective, this behaviour can be

explained by the fact that an increase in permeability enhances the fluid's ability to pass through the porous medium which increases heat transfer properties.

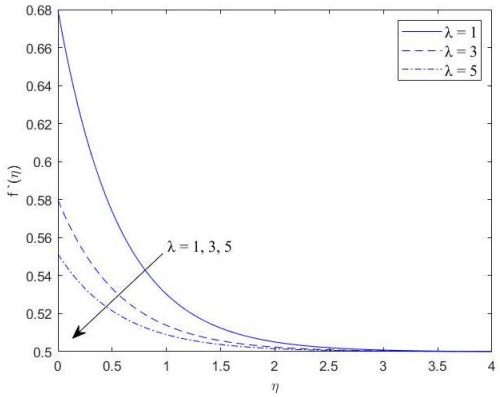

Figure 6: Velocity profile $f'(0)$ for different values of λ when Pr = 0.7, A = 1, δ = 1, b = 0.5 and K = 1.

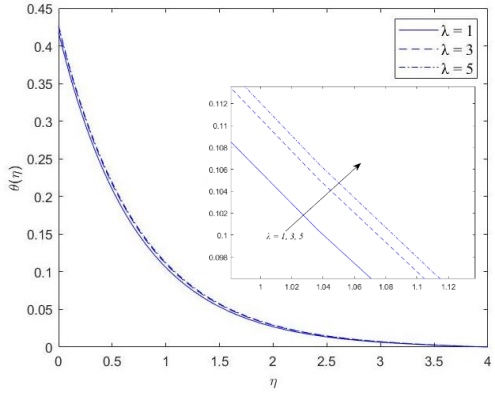

Figure 7: Temperature profile $\theta(0)$ for different values of λ when Pr = 0.7, A = 1, δ = 1, b = 0.5 and K = 1.

Figure 6 and Figure 7 show the influence of various velocity slip parameter λ on velocity and temperature profiles. Figure 6 illustrated that the fluid velocity decrease when the velocity slip parameter λ increase. This is because when velocity slip occurs, the velocity of fluid flow close to the surface is no longer equal to the velocity stretching surface. Therefore, physically this slips condition represents as a surface with partial resistance towards the fluid movement in porous medium. Moreover, the result from Figure 7 discovered that the temperature profile exhibits an increasing pattern as the values of λ increase. Higher values of λ indicate greater slip at the surface, leading to enhanced heat transfer from the surface to the fluid due to lower tangential velocity. The temperature distribution is indirectly influenced by the velocity slip parameter λ, which modifies the fluid flow close to the surface.

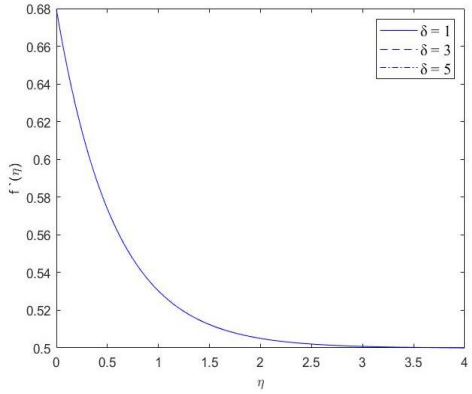

Figure 8: Velocity profile $f'(0)$ for different values of δ when Pr = 0.7, A = 1, b = 0.5, K = 1 and λ = 1.

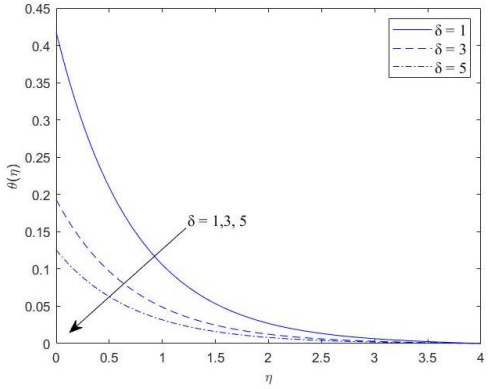

Figure 9: Temperature profile $\theta(0)$ for different values of δ when Pr = 0.7, A = 1, b = 0.5, K = 1 and λ = 1.

Figure 8 and Figure 9 show the influence of various thermal slip parameter δ on velocity and temperature profiles. From Figure 8, it can be seen that by increasing values of the thermal slip parameter δ, the velocity profile does not change and remain constant. This shows that the thermal slip parameter has no observable effect on the velocity profile. This could occur when momentum diffusion dominates over thermal effects, meaning the velocity field is primarily governed by the momentum boundary conditions rather than thermal slip effects. Figure 9 indicates that the temperature profile decreases due to increasing values of thermal slip parameter δ. Higher δ reduces the effectiveness of heat transfer between the boundary and the fluid, leading to a thinner thermal boundary layer. Physically, this means that the temperature changes more rapidly near the boundary and the thermal influence does not extend far into the fluid.

4. Conclusion

This study investigates the unsteady boundary layer flow of a stretching sheet over a porous medium. The boundary layer flow equations in nonlinear partial differential equations have been transformed into dimensionless ordinary differential equations through similarity transformation. Then, the equations are solved numerically using BVP4C method in MATLAB software. Hence, the results that are obtained as follows:

i. The velocity profile $f'(0)$ decrease as the increasing values of permeability parameter K and velocity slip parameter λ.

ii. The velocity profile $f'(0)$ constant when thermal slip parameter δ increases.

iii. The temperature profile $\theta(0)$ decrease with the increasing values of permeability parameter K and thermal slip parameter δ.

iv. The temperature profile $\theta(0)$ increase when velocity slip parameter λ increases.

v. The skin friction coefficient $f''(0)$ decreases due to increasing permeability parameter K.

vi. The skin friction coefficient $f''(0)$ increases with the increasing velocity slip parameter λ.

vii. The local Nusselt number $-\theta'(0)$ increase when permeability parameter K increase.

viii. The local Nusselt number $-\theta'(0)$ decrease as velocity slip λ and thermal slip parameter δ increases.

Acknowledgments

The authors would like to express their sincere gratitude to Universiti Teknologi MARA (UiTM) for providing the necessary facilities and resources to conduct this research. Special appreciation is extended to the College of Computing, Informatics and Mathematics for their continuous support and valuable guidance.

References

[1] Tani, I. (1977). History of boundary layer theory. *Annual Review of Fluid Mechanics*, *9*(1), 87–111. https://doi.org/10.1146/annurev.fl.09.010177.000511

[2] Kamrava, S., Sahimi, M., & Tahmasebi, P. (2021). Simulating fluid flow in complex porous materials by integrating the governing equations with deep-layered machines. Npj Computational Materials, 7(1). https://doi.org/10.1038/s41524-021-00598-2

[3] Sudarmozhi, K., Iranian, D., & Alessa, N. (2024). Investigation of melting heat effect on fluid flow with brownian motion/thermophoresis effects in the occurrence of energy on a stretching sheet. *Alexandria Engineering Journal /Alexandria Engineering Journal*, *94*, 366–376. https://doi.org/10.1016/j.aej.2024.03.065

[4] Zhou, J., Abidi, A., Shi, Q., Khan, M. R., Rehman, A., Issakhov, A., & Galal, A. M. (2021). Unsteady radiative slip flow of MHD Casson fluid over a permeable stretched surface subject to a non-uniform heat source. *Case Studies in Thermal Engineering*, *26*, 101141. https://doi.org/10.1016/j.csite.2021.101141

[5] Verma, A. K., Rajput, S., Bhattacharyya, K., & Chamkha, A. J. (2022). Nanoparticle's radius effect on unsteady mixed convective copper-water nanofluid flow over an expanding sheet in porous medium with boundary slip. *Chemical Engineering Journal Advances*, *12*, 100366. https://doi.org/10.1016/j.ceja.2022.100366

[6] Goud, B. S., Kumar, P. P., & Malga, B. S. (2020). Effect of Heat source on an unsteady MHD free convection flow of Casson fluid past a vertical oscillating plate in porous medium using finite element analysis. *Partial Differential Equations in Applied Mathematics*, *2*, 100015. https://doi.org/10.1016/j.padiff.2020.100015

[7] Rao, S. R., Vidyasagar, G., & Deekshitulu, G. (2021). Unsteady MHD free convection Casson fluid flow past an exponentially accelerated infinite vertical porous plate through porous medium in the presence of radiation absorption with heat generation/absorption. *Materials Today: Proceedings*, *42*, 1608–1616. https://doi.org/10.1016/j.matpr.2020.07.554

[8] Mandal, S., & Shit, G. (2021). Entropy analysis on unsteady MHD biviscosity nanofluid flow with convective heat transfer in a permeable radiative stretchable rotating disk. *Chinese*

Journal of Physics/Zhōngguó Wùlǐ Xuékān, *74*, 239–255. https://doi.org/10.1016/j.cjph.2021.07.036

[9] Marinca, B., Herişanu, N., & Marinca, V. (2023). Analytical solutions for solving unsteady flow of gas through a porous medium by using auxiliary functions method. *Journal of Computational and Applied Mathematics*, *432*, 115296. https://doi.org/10.1016/j.cam.2023.115296

[10] Almalki, F. M. K., & Meylan, M. H. (2024). Analytic solution of the free boundary problem for porous media flow using a conformal map validated by the boundary element method. *Engineering Analysis with Boundary Elements*, *166*, 105806. https://doi.org/10.1016/j.enganabound.2024.105806

[11] Fahim, M., Sajid, M., Ali, N., & Naveed, M. (2023). Unsteady blood flow of Carreau fluid in a porous saturated medium with stenosis under the influence of acceleration and magnetic fields: A comprehensive analysis. *Computers in Biology and Medicine*, *164*, 107278. https://doi.org/10.1016/j.compbiomed.2023.107278

[12] Goud, B. S., Srilatha, P., Srinivasulu, T., Reddy, Y. D., & Kumar, K. S. (2023). Induced by heat source on unsteady MHD free convective flow of Casson fluid past a vertically oscillating plate through porous medium utilizing finite difference method. *Materials Today: Proceedings*. https://doi.org/10.1016/j.matpr.2023.01.378

[13] Preetham, M., Kumbinarasaiah, S., & Alshehri, M. (2024). Application of Fibonacci wavelet in the analysis of unsteady MHD Williamson nanofluid flow over a permeable stretching sheet via porous medium. *Results in Physics*, 107853. https://doi.org/10.1016/j.rinp.2024.107853

[14] Khan, D., Ali, G., Kumam, P., Sitthithakerngkiet, K., & Jarad, F. (2023). Heat transfer analysis of unsteady MHD slip flow of ternary hybrid Casson fluid through nonlinear stretching disk embedded in a porous medium. *Ain Shams Engineering Journal/Ain Shams Engineering Journal*, *15*(2), 102419. https://doi.org/10.1016/j.asej.2023.102419

[15] Zegeye, G. B., Haile, E., & Awgichew, G. (2024). Viscous dissipation and Joule heating effects of Carreau nanofluid axisymmetric flow past unsteady radially stretching porous disk. *International Journal of Thermofluids*, *22*, 100655. https://doi.org/10.1016/j.ijft.2024.100655

[16] Waqas, H., Farooq, U., Liu, D., Alghamdi, M., Noreen, S., & Muhammad, T. (2022). Numerical investigation of nanofluid flow with gold and silver nanoparticles injected inside a stenotic artery. *Materials & Design*, *223*, 111130. https://doi.org/10.1016/j.matdes.2022.111130

[17] Zada, L., Ullah, I., Alqahtani, A. M., Nawaz, R., Khan, H., & Alam, K. (2024). Enhancing energy efficiency and heat transfer performance of engine oil flow through hybrid nanoparticles in convergent/divergent channel. *Results in Engineering*, *22*, 102027. https://doi.org/10.1016/j.rineng.2024.102027

[18] Rosali, H., Badlilshah, M. N., Johari, M. a. M., & Bachok, N. (2020). Unsteady Boundary Layer Stagnation Point Flow and Heat Transfer over a Stretching Sheet in a Porous Medium with Slip Effects. *CFD Letters*, *12*(10), 52–61. https://doi.org/10.37934/cfdl.12.10.5261